First-Principles Calculation of Electric Polarization

Fumiyuki Ishii
Kanazawa University

The International Summer workShop 2018
on First-Principles Electronic Structure Calculations (ISS2018), July 5, 2018

Electric polarization

- Fundamental physical quantity of insulators
- Characterize dielectric properties of insulators
- Piezoelectricity, Ferroelectricity, Magnetoelectric effect
- Many applications
  - Capacitor, Piezoelectric device, Ferroelectric memory
- Momentum dependence: Characterize topological insulators

Perturbations and Responses

Perturbations / Responses	1. Mecanical 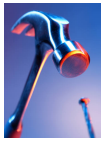	2. Thermal 	3. Electric 	4. Magnetic 	5. Chemical 
1. Mecanical	Elasticity	Thermal expansion	Electromechanical	Magnetostriction	Osmotic pressure
2. Thermal	Thermal insulating	Thermal conductivity	Pyroelectric/ Thermoelectric (Peltier)	Thermomagnetic	Heat diffusion
3. Electric	Piezoelectric	Pyroelectric/ Thermoelectric (Seebeck)	Electric Polarization Electric Conductivity	Magnetoelectric	Battery
4. Magnetic	Magnetostriction	Thermomagnetic	Magnetoelectric	Magnetization	?
5. Chemical	Osmotic pressure	Heat diffusion	Battery	?	diffusion

Based on the table of Hidetoshi Takahashi

In the textbook /

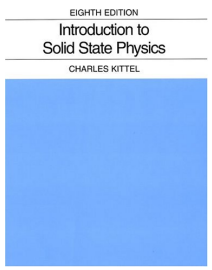

The polarization P is defined as the dipole moment per unit volume, averaged over the volume of a cell.

$$\mathbf{P} = \frac{1}{V_s}\sum_{i}^{s}\mathbf{p}_i = \frac{1}{V_s}\sum_{n}^{s}\mathbf{r}_n q$$

$$= \frac{1}{V_c}\sum_{n}^{c}\mathbf{r}_n q_n$$

S:sample ,C:cell

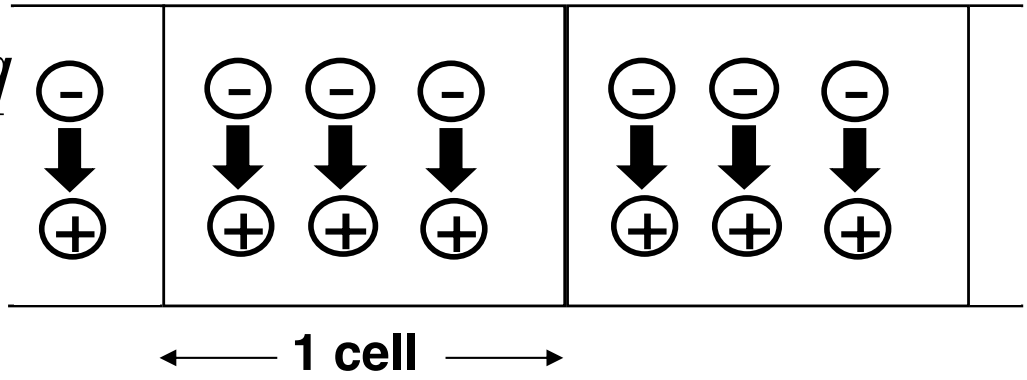

Periodic boundary condition

Dipole sum of discrete charges

Problems in electric polarization

- **Resta (1992):**

  Contrary to common textbook statements, the dipole of a periodic charge distribution is ill defined, except the case in which the total charge is unambiguously decomposed into an assembly of localized and neutral charge distributions.

  P is not a bulk property, while the variations of P are indeed measurable.

Can we compute *P* from charge density ?

Charge distribution is continuous in real materials.

R. M. Martin, PRB 9, 1998(1974).

Local polarization field $\mathbf{P}_{el}(\mathbf{r})$

$$\nabla \cdot \mathbf{P}_{el}(\mathbf{r}) = -\rho(\mathbf{r})$$

$$\mathbf{P}_{el} = \frac{1}{\Omega}\int_{cell} \mathbf{P}(\mathbf{r})d\mathbf{r}$$

$$= \frac{1}{\Omega}\int_{cell} d\mathbf{r}\rho(\mathbf{r})\mathbf{r} + \frac{1}{\Omega}\int_{surface} \mathbf{r}[\mathbf{n}\cdot\mathbf{P}(\mathbf{r})]ds$$

cell to cell term (current)

Conclusion :

- **Absolute value of polarization is not bulk property**
- **Dipole moment divided by unit cell volume → Polarization**

Observation of electric polarization

- Current induced by perturbation

$$\mathbf{J}(\lambda) = \frac{\partial \mathbf{P}}{\partial \lambda}$$

- Change in polarization by perturbation

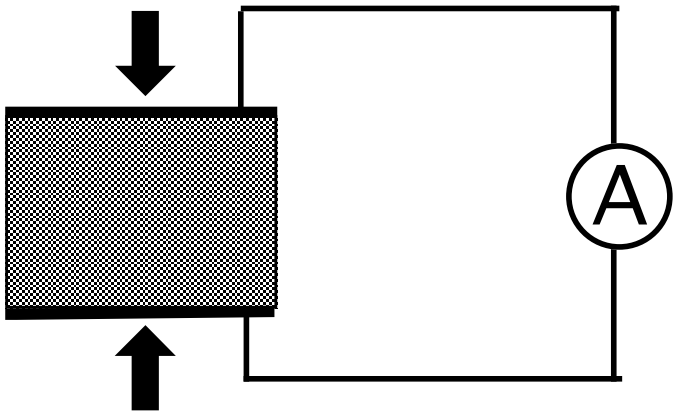

$$\Delta \mathbf{P} = \int \mathbf{J}(\lambda) d\lambda = \int \frac{\partial \mathbf{P}}{\partial \lambda} d\lambda$$

In classical way:

$$\mathbf{j} = -ne\mathbf{v}$$

$$\Delta \mathbf{P} = \int_0^{\Delta t} -ne\mathbf{v}dt = [-ne\mathbf{r}(\Delta t)] - [-ne\mathbf{r}(0)]$$

$$= \mathbf{P}(\Delta t) - \mathbf{P}(0)$$

Electric polarization expressed by wave function

$$\boldsymbol{P} = \frac{e}{V}\sum_{\boldsymbol{k}}\sum_{n=1}^{occ}\langle\psi_n^{\boldsymbol{k}}|\boldsymbol{r}|\psi_n^{\boldsymbol{k}}\rangle$$

$$H|\psi_n^{\boldsymbol{k}}\rangle = E_n^{\boldsymbol{k}}|\psi_n^{\boldsymbol{k}}\rangle$$

$$\begin{aligned}
\frac{d\boldsymbol{P}}{dt} &= \frac{e}{V}\sum_{\boldsymbol{k}}\sum_{n=1}^{occ}\frac{d}{dt}\langle\psi_n^{\boldsymbol{k}}|\boldsymbol{r}|\psi_n^{\boldsymbol{k}}\rangle \\
&= \frac{e}{V}\sum_{\boldsymbol{k}}\sum_{n=1}^{occ}\left(\langle\partial_t\psi_n^{\boldsymbol{k}}|\boldsymbol{r}|\psi_n^{\boldsymbol{k}}\rangle + \langle\psi_n^{\boldsymbol{k}}|\boldsymbol{r}|\partial_t\psi_n^{\boldsymbol{k}}\rangle\right) \\
&= \frac{e}{V}\sum_{\boldsymbol{k}}\sum_{n=1}^{occ}\sum_{m=1}^{\infty}(\langle\partial_t\psi_n^{\boldsymbol{k}}|\psi_m^{\boldsymbol{k}}\rangle\langle\psi_m^{\boldsymbol{k}}|\boldsymbol{r}|\psi_n^{\boldsymbol{k}}\rangle \\
&+ \langle\psi_n^{\boldsymbol{k}}|\boldsymbol{r}|\psi_m^{\boldsymbol{k}}\rangle\langle\psi_m^{\boldsymbol{k}}|\partial_t\psi_n^{\boldsymbol{k}}\rangle)
\end{aligned}$$

Electric polarization expressed by wave function

$$\begin{aligned}\frac{d\boldsymbol{P}}{dt} &= \frac{e}{V}\sum_{\boldsymbol{k}}\sum_{n=1}^{occ}\sum_{m=1}^{\infty}(\langle\partial_t\psi_n^{\boldsymbol{k}}|\psi_m^{\boldsymbol{k}}\rangle\langle\psi_m^{\boldsymbol{k}}|\boldsymbol{r}|\psi_n^{\boldsymbol{k}}\rangle \\ &+ \langle\psi_n^{\boldsymbol{k}}|\boldsymbol{r}|\psi_m^{\boldsymbol{k}}\rangle\langle\psi_m^{\boldsymbol{k}}|\partial_t\psi_n^{\boldsymbol{k}}\rangle)\end{aligned}$$

Velocity operator

$$\begin{aligned}\langle\psi_m^{\boldsymbol{k}}|\boldsymbol{v}|\psi_n^{\boldsymbol{k}}\rangle &= i\hbar\langle\psi_m^{\boldsymbol{k}}|[\boldsymbol{r},H]|\psi_n^{\boldsymbol{k}}\rangle = i\hbar(E_n^{\boldsymbol{k}}-E_m^{\boldsymbol{k}})\langle\psi_m^{\boldsymbol{k}}|\boldsymbol{r}|\psi_n^{\boldsymbol{k}}\rangle \\ \langle\psi_m^{\boldsymbol{k}}|\boldsymbol{r}|\psi_n^{\boldsymbol{k}}\rangle &= \frac{\langle\psi_m^{\boldsymbol{k}}|\boldsymbol{v}|\psi_n^{\boldsymbol{k}}\rangle}{i\hbar(E_n^{\boldsymbol{k}}-E_m^{\boldsymbol{k}})} \\ \langle\psi_n^{\boldsymbol{k}}|\boldsymbol{r}|\psi_m^{\boldsymbol{k}}\rangle &= (\langle\psi_m^{\boldsymbol{k}}|\boldsymbol{r}|\psi_n^{\boldsymbol{k}}\rangle)^*\end{aligned}$$

Electric polarization expressed by wave function

$$\frac{d\boldsymbol{P}}{dt} = \frac{-ie}{V\hbar}\sum_{\boldsymbol{k}}\sum_{n=1}^{occ}\sum_{m\neq n}\left(\frac{\langle\partial_t\psi_n^{\boldsymbol{k}}|\psi_m^{\boldsymbol{k}}\rangle\langle\psi_m^{\boldsymbol{k}}|v|\psi_n^{\boldsymbol{k}}\rangle}{(E_n^{\boldsymbol{k}}-E_m^{\boldsymbol{k}})} - c.c\right)$$

Bloch wavefunction and its periodic part

$$\begin{aligned}
|\psi_n^{\boldsymbol{k}}\rangle &= e^{i\boldsymbol{k}\cdot\boldsymbol{r}}|u_n^{\boldsymbol{k}}\rangle \\
H|\psi_n^{\boldsymbol{k}}\rangle &= E_n^{\boldsymbol{k}}|\psi_n^{\boldsymbol{k}}\rangle \\
e^{-i\boldsymbol{k}\cdot\boldsymbol{r}}He^{i\boldsymbol{k}\cdot\boldsymbol{r}}|u_n^{\boldsymbol{k}}\rangle &= E_n^{\boldsymbol{k}}|u_n^{\boldsymbol{k}}\rangle \\
\tilde{H}|u_n^{\boldsymbol{k}}\rangle &= E_n^{\boldsymbol{k}}|u_n^{\boldsymbol{k}}\rangle \\
\langle\psi_m^{\boldsymbol{k}}|v|\psi_n^{\boldsymbol{k}}\rangle &= \langle u_m^{\boldsymbol{k}}|\tilde{v}|u_n^{\boldsymbol{k}}\rangle
\end{aligned}$$

Heisenberg Equation of Motion

$$
\begin{aligned}
i\hbar\frac{dr}{dt} &= [r, H] \\
i\hbar v &= [r, H]
\end{aligned}
$$

Bloch wavefunction and its periodic part

$$
\begin{aligned}
\tilde{H} &= e^{-ik\cdot r} H e^{ik\cdot r} \\
e^{-ik\cdot r}[r, H]e^{ik\cdot r} &= e^{-ik\cdot r}\left(i\hbar\frac{dr}{dt}\right)e^{ik\cdot r} = i\hbar\tilde{v}
\end{aligned}
$$

if $[\nabla_k, H] = 0$,

$$
\begin{aligned}
\nabla_k\tilde{H} &= -ire^{-ik\cdot r} H e^{ik\cdot r} + e^{-ik\cdot r} H e^{ik\cdot r} ir \\
\nabla_k\tilde{H} &= -i[r, \tilde{H}] = \hbar\tilde{v} \\
\langle\psi_m^k|v|\psi_n^k\rangle &= \langle u_m^k|\tilde{v}|u_n^k\rangle = \langle u_m^k|\frac{\nabla_k\tilde{H}}{\hbar}|u_n^k\rangle
\end{aligned}
$$

Electric polarization expressed by wave function

$$
\begin{aligned}
\frac{d\boldsymbol{P}}{dt} &= \frac{-ie}{8\pi^3\hbar}\int_{BZ} d\boldsymbol{k} \sum_{n=1}^{occ}\sum_{m\neq n}\left(\frac{\langle\partial_t\psi_n^{\boldsymbol{k}}|\psi_m^{\boldsymbol{k}}\rangle\langle\psi_m^{\boldsymbol{k}}|v|\psi_n^{\boldsymbol{k}}\rangle}{(E_n^{\boldsymbol{k}}-E_m^{\boldsymbol{k}})} - c.c\right) \\
&= \frac{-ie}{8\pi^3\hbar}\int_{BZ} d\boldsymbol{k} \sum_{n=1}^{occ}\sum_{m\neq n}\left(\frac{\langle\partial_t u_n^{\boldsymbol{k}}|u_m^{\boldsymbol{k}}\rangle\langle u_m^{\boldsymbol{k}}|\tilde{v}|u_n^{\boldsymbol{k}}\rangle}{(E_n^{\boldsymbol{k}}-E_m^{\boldsymbol{k}})} - c.c\right) \\
&= \frac{-ie}{8\pi^3}\int_{BZ} d\boldsymbol{k} \sum_{n=1}^{occ}\sum_{m\neq n}\left(\frac{\langle\partial_t u_n^{\boldsymbol{k}}|u_m^{\boldsymbol{k}}\rangle\langle u_m^{\boldsymbol{k}}|\nabla_{\boldsymbol{k}}\tilde{H}|u_n^{\boldsymbol{k}}\rangle}{(E_n^{\boldsymbol{k}}-E_m^{\boldsymbol{k}})} - c.c\right) \\
&= \frac{-ie}{8\pi^3}\int_{BZ} d\boldsymbol{k} \sum_{n=1}^{occ}\left(\langle\partial_t u_n^{\boldsymbol{k}}|\nabla_{\boldsymbol{k}}u_n^{\boldsymbol{k}}\rangle - \langle\nabla_{\boldsymbol{k}}u_n^{\boldsymbol{k}}|\partial_t u_n^{\boldsymbol{k}}\rangle\right)
\end{aligned}
$$

First-order perturbation theory

$$
\begin{aligned}
\delta\tilde{H} &= \tilde{H}(k+\Delta k) - \tilde{H}(k) \\
|u_n^{k+\Delta k}\rangle &= |u_n^k\rangle \\
&+ \sum_{m\neq n} |u_m^k\rangle \frac{\langle u_m^k|\delta\tilde{H}|u_n^k\rangle}{E_n^k - E_m^k} + O(\delta\tilde{H}^2) \\
|\nabla_k u_n^k\rangle &\simeq \sum_{m\neq n} |u_m^k\rangle \frac{\langle u_m^k|\nabla_k\tilde{H}|u_n^k\rangle}{E_n^k - E_m^k}
\end{aligned}
$$

Ordinary derivative to partial derivative

$$
\frac{d}{dt}|u_{k_\alpha,t}\rangle = \partial_{k_\alpha}|u_{k_\alpha,t}\rangle\frac{dk_\alpha}{dt} + \partial_t|u_{k_\alpha,t}\rangle = \partial_t|u_{k_\alpha,t}\rangle
$$

Electric polarization expressed by wave function

$$\int_0^{\Delta t} dt \frac{d\boldsymbol{P}}{dt} = \boldsymbol{P}(\Delta t) - \boldsymbol{P}(0)$$

$$= \frac{-ie}{8\pi^3} \int_0^{\Delta t} dt \int_{BZ} d\boldsymbol{k} \sum_{n=1}^{occ} \left(\langle \partial_t u_n^{\boldsymbol{k}} | \nabla_{\boldsymbol{k}} u_n^{\boldsymbol{k}} \rangle - \langle \nabla_{\boldsymbol{k}} u_n^{\boldsymbol{k}} | \partial_t u_n^{\boldsymbol{k}} \rangle \right)$$

$$= \frac{-ie}{8\pi^3} \int_0^{\Delta t} dt \int_{BZ} d\boldsymbol{k} \sum_{n=1}^{occ} \left(\partial_t \langle u_n^{\boldsymbol{k}} | \nabla_{\boldsymbol{k}} u_n^{\boldsymbol{k}} \rangle - \nabla_{\boldsymbol{k}} \langle u_n^{\boldsymbol{k}} | \partial_t u_n^{\boldsymbol{k}} \rangle \right)$$

For k_α direction,

$$P_\alpha(\Delta t) - P_\alpha(0)$$

$$= \frac{ie}{8\pi^3} \int dk_\beta dk_\gamma \times$$

$$\int_0^{\Delta t} dt \int_0^{G_\alpha} dk_\alpha \sum_{n=1}^{occ} \left(\partial_{k_\alpha} \langle u_n^{\boldsymbol{k}} | \partial_t u_n^{\boldsymbol{k}} \rangle - \partial_t \langle u_n^{\boldsymbol{k}} | \partial_{k_\alpha} u_n^{\boldsymbol{k}} \rangle \right)$$

Electric polarization expressed by Berry phase
(King-Smith & Vanderbilt 1993)

$$P_\alpha(t) = \frac{-ie}{8\pi^3} \int dk_\beta dk_\gamma \sum_{n=1}^{occ} \int_0^{G_\alpha} dk_\alpha \langle u_n^{\boldsymbol{k}}(t) | \partial_{k_\alpha} | u_n^{\boldsymbol{k}}(t) \rangle$$

$$= \frac{e}{8\pi^3} \int dk_\beta dk_\gamma \sum_{n=1}^{occ} \mathrm{Im} \int_0^{G_\alpha} dk_\alpha \langle u_n^{\boldsymbol{k}}(t) | \partial_{k_\alpha} | u_n^{\boldsymbol{k}}(t) \rangle$$

Example: Orthorhombic unitcell

Case: $(k_\beta, k_\gamma) = (0,0)$ sampling , $G_\beta = \frac{2\pi}{b}$, $G_\gamma = \frac{2\pi}{c}$

$$
\begin{aligned}
P_\alpha(t) &= \frac{e}{8\pi^3} \int dk_\beta dk_\gamma \sum_{n=1}^{occ} \mathrm{Im} \int_0^{G_\alpha} dk_\alpha \langle u_n^{\boldsymbol{k}}(t) | \partial_{k_\alpha} | u_n^{\boldsymbol{k}}(t) \rangle \\
&= \frac{e}{8\pi^3} \int dk_\beta dk_\gamma \phi(t) \\
&= \frac{e}{8\pi^3} \frac{2\pi}{b} \frac{2\pi}{c} \phi(t) = \frac{e}{2\pi bc} \phi(t) = \frac{ea}{2\pi abc} \phi(t) \\
&= \frac{ea}{2\pi \Omega_{cell}} \phi(t) = \frac{ea}{\Omega_{cell}} \left(\frac{\phi(t)}{2\pi} \right)
\end{aligned}
$$

Numerical calculation of Berry Phase

- $A = \log S \leftrightarrow \exp A = S$
- $\det \exp A = \exp \mathrm{tr}\, A$, $\log \det S = \mathrm{tr} \log S$
- $S_{nm}(\boldsymbol{k}, \boldsymbol{k}')|_{\boldsymbol{k}=\boldsymbol{k}'} = \delta_{mn}$

$$
\begin{aligned}
\phi(t) &= \mathrm{Im} \int_0^{G_\alpha} dk_\alpha \mathrm{tr} \partial_{k'_\alpha} S(\boldsymbol{k}, \boldsymbol{k}')|_{\boldsymbol{k}=\boldsymbol{k}'} \\
&= \mathrm{Im} \int_0^{G_\alpha} dk_\alpha \mathrm{tr} \left[\frac{\partial_{k'_\alpha} S(\boldsymbol{k}, \boldsymbol{k}')}{S(\boldsymbol{k}, \boldsymbol{k}')} \right]_{|\boldsymbol{k}=\boldsymbol{k}'} \\
&= \mathrm{Im} \int_0^{G_\alpha} dk_\alpha \mathrm{tr} \partial_{k'_\alpha} \log\, S(\boldsymbol{k}, \boldsymbol{k}')|_{\boldsymbol{k}=\boldsymbol{k}'} \\
&= \mathrm{Im} \int_0^{G_\alpha} dk_\alpha \partial_{k'_\alpha} \log \det S(\boldsymbol{k}, \boldsymbol{k}')|_{\boldsymbol{k}=\boldsymbol{k}'}
\end{aligned}
$$

Numerical calculation of Berry Phase

- $A = \log S \leftrightarrow \exp A = S$
- $\det \exp A = \exp \mathrm{tr}\, A$, $\log \det S = \mathrm{tr} \log S$
- $S_{nm}(\boldsymbol{k}, \boldsymbol{k}', t)|_{\boldsymbol{k}=\boldsymbol{k}'} = \delta_{mn}$

$$
\begin{aligned}
\phi(t) &= \mathrm{Im} \int_0^{G_\alpha} dk_\alpha \mathrm{tr} \partial_{k'_\alpha} S(\boldsymbol{k}, \boldsymbol{k}', t)|_{\boldsymbol{k}=\boldsymbol{k}'} \\
&= \mathrm{Im} \int_0^{G_\alpha} dk_\alpha \mathrm{tr} \left[\frac{\partial_{k'_\alpha} S(\boldsymbol{k}, \boldsymbol{k}', t)}{S(\boldsymbol{k}, \boldsymbol{k}', t)} \right]_{|\boldsymbol{k}=\boldsymbol{k}'} \\
&= \mathrm{Im} \int_0^{G_\alpha} dk_\alpha \mathrm{tr} \partial_{k'_\alpha} \log\, S(\boldsymbol{k}, \boldsymbol{k}', t)|_{\boldsymbol{k}=\boldsymbol{k}'} \\
&= \mathrm{Im} \int_0^{G_\alpha} dk_\alpha \partial_{k'_\alpha} \log \det S(\boldsymbol{k}, \boldsymbol{k}', t)|_{\boldsymbol{k}=\boldsymbol{k}'}
\end{aligned}
$$

Numerical calculation of Berry Phase

$$\phi(t) = \mathrm{Im} \int_0^{G_\alpha} dk_\alpha \partial_{k'_\alpha} \log \det S(\boldsymbol{k}, \boldsymbol{k}', t)|_{\boldsymbol{k}=\boldsymbol{k}'}$$

If we use k-point sampling mesh J along k_α direction, $k_{\alpha,s} = sG_\alpha/J$ and $\Delta k_\alpha = G_\alpha/\mathrm{J}$.

$$\phi(t) = \mathrm{Im} \lim_{\Delta k_\alpha \to 0} \sum_{s=0}^{J-1} \Delta k_\alpha \times$$

$$\frac{\log \det S_{nm}(k_{\alpha,s}, k_{\alpha,s} + \Delta k_\alpha, t) - \log \det S_{nm}(k_{\alpha,s}, k_{\alpha,s}, t)}{\Delta k_\alpha}$$

$$\phi(t) = \mathrm{Im} \lim_{\Delta k_\alpha \to 0} \sum_{s=0}^{J-1} \log \det S_{nm}(k_{\alpha,s} k_{\alpha,s} + \Delta k_\alpha, t)$$

Numerical calculation of Berry Phase

$$\begin{aligned}\phi(t) &= \mathrm{Im} \lim_{\Delta k_\alpha \to 0} \sum_{s=0}^{J-1} \log \det S_{nm}(k_{\alpha,s} k_{\alpha,s} + \Delta k_\alpha, t) \\ &= \mathrm{Im} \lim_{\Delta k_\alpha \to 0} \log \prod_{s=0}^{J-1} \det S_{nm}(k_{\alpha,s} k_{\alpha,s} + \Delta k_\alpha, t)\end{aligned}$$

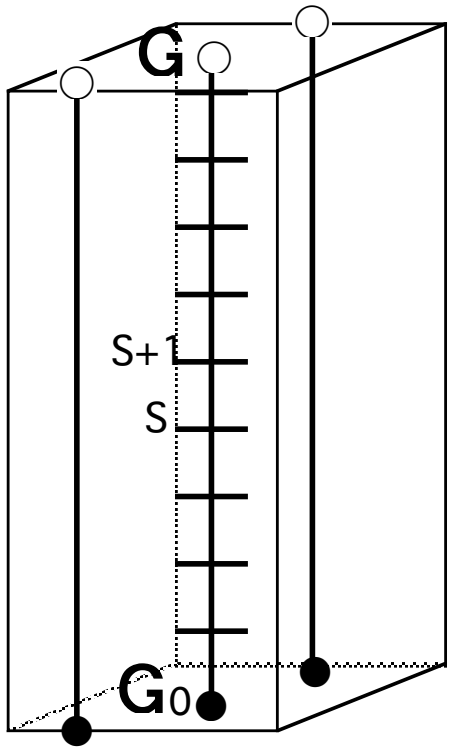

Overlap matrix *S* in OpenMX

$$
\begin{aligned}
\psi^{(\mathbf{k})}_{\sigma\mu}(\mathbf{r}) &= \mathrm{e}^{\mathrm{i}\mathbf{k}\cdot\mathbf{r}} u^{(\mathbf{k})}_{\sigma\mu}(\mathbf{r}), \\
&= \frac{1}{\sqrt{N}} \sum_{\mathrm{n}}^{N} \mathrm{e}^{\mathrm{i}\mathbf{R}_{\mathrm{n}}\cdot\mathbf{k}} \sum_{i\alpha} c^{(\mathbf{k})}_{\sigma\mu,i\alpha} \phi_{i\alpha}(\mathbf{r}-\tau_i-\mathbf{R}_{\mathrm{n}}),
\end{aligned}
$$

$$
\begin{aligned}
\langle u^{(\mathbf{k})}_{\sigma\mu} | u^{(\mathbf{k}+\Delta\mathbf{k})}_{\sigma\nu} \rangle &= \langle \psi^{(\mathbf{k})}_{\sigma\mu} | \mathrm{e}^{\mathrm{i}\mathbf{k}\cdot\mathbf{r}} \mathrm{e}^{-\mathrm{i}\mathbf{k}\cdot\mathbf{r}} \mathrm{e}^{-\mathrm{i}\Delta\mathbf{k}\cdot\mathbf{r}} | \psi^{(\mathbf{k}+\boldsymbol{\Delta}\mathbf{k})}_{\sigma\nu} \rangle, \\
&= \langle \psi^{(\mathbf{k})}_{\sigma\mu} | \mathrm{e}^{-\mathrm{i}\Delta\mathbf{k}\cdot\mathbf{r}} | \psi^{(\mathbf{k}+\boldsymbol{\Delta}\mathbf{k})}_{\sigma\nu} \rangle, \\
&= \frac{1}{N} \sum_{\mathrm{n},\mathrm{n}'} \sum_{i\alpha,j\beta} c^{(\mathbf{k})*}_{\sigma\mu,i\alpha} c^{(\mathbf{k}+\boldsymbol{\Delta}\mathbf{k})}_{\sigma\nu,j\beta} \mathrm{e}^{-\mathrm{i}\mathbf{k}\cdot(\mathbf{R}_{\mathrm{n}}-\mathbf{R}_{\mathrm{n}'})} \times \\
&\quad \langle \phi_{i\alpha}(\mathbf{r}-\tau_i-\mathbf{R}_{\mathrm{n}}) | \mathrm{e}^{-\mathrm{i}\Delta\mathbf{k}\cdot(\mathbf{r}-\mathbf{R}_{\mathrm{n}'})} | \phi_{j\beta}(\mathbf{r}-\tau_j-\mathbf{R}_{\mathrm{n}'}) \rangle.
\end{aligned}
$$

$$
\mathbf{r}' = \mathbf{r} - \tau_i - \mathbf{R}_{\mathrm{n}},
$$

Overlap matrix *S* in OpenMX

$$\langle u^{(\mathbf{k})}_{\sigma\mu}|u^{(\mathbf{k}+\Delta\mathbf{k})}_{\sigma\nu}\rangle = \frac{1}{N}\sum_{\mathrm{n},\mathrm{n}'}\sum_{i\alpha,j\beta} c^{(\mathbf{k})*}_{\sigma\mu,i\alpha}c^{(\mathbf{k}+\boldsymbol{\Delta}\mathbf{k})}_{\sigma\nu,j\beta}\mathrm{e}^{-\mathrm{i}\mathbf{k}\cdot(\mathbf{R}_\mathrm{n}-\mathbf{R}_{\mathrm{n}'})}\times \langle\phi_{i\alpha}(\mathbf{r}')|\mathrm{e}^{-\mathrm{i}\Delta\mathbf{k}\cdot(\mathbf{r}'+\tau_i+\mathbf{R}_\mathrm{n}-\mathbf{R}_{\mathrm{n}'})}|\phi_{j\beta}(\mathbf{r}'+\tau_i-\tau_j+\mathbf{R}_\mathrm{n}-\mathbf{R}_{\mathrm{n}'})\rangle.$$

$$\begin{aligned}\langle u^{(\mathbf{k})}_{\sigma\mu}|u^{(\mathbf{k}+\Delta\mathbf{k})}_{\sigma\nu}\rangle &= \sum_{\mathrm{n}}\sum_{i\alpha,j\beta} c^{(\mathbf{k})*}_{\sigma\mu,i\alpha}c^{(\mathbf{k}+\boldsymbol{\Delta}\mathbf{k})}_{\sigma\nu,j\beta}\mathrm{e}^{\mathrm{i}\mathbf{k}\cdot\mathbf{R}_\mathrm{n}}\times\langle\phi_{i\alpha}(\mathbf{r}')|\mathrm{e}^{-\mathrm{i}\Delta\mathbf{k}\cdot(\mathbf{r}'+\tau_i-\mathbf{R}_\mathrm{n})}|\phi_{j\beta}(\mathbf{r}'+\tau_i-\tau_j-\mathbf{R}_\mathrm{n})\rangle,\\ &= \sum_{\mathrm{n}}\sum_{i\alpha,j\beta} c^{(\mathbf{k})*}_{\sigma\mu,i\alpha}c^{(\mathbf{k}+\boldsymbol{\Delta}\mathbf{k})}_{\sigma\nu,j\beta}\mathrm{e}^{\mathrm{i}\mathbf{k}\cdot\mathbf{R}_\mathrm{n}}\mathrm{e}^{-\mathrm{i}\Delta\mathbf{k}\cdot(\tau_i-\mathbf{R}_\mathrm{n})}\langle\phi_{i\alpha}(\mathbf{r}')|\mathrm{e}^{-\mathrm{i}\Delta\mathbf{k}\cdot\mathbf{r}'}|\phi_{j\beta}(\mathbf{r}'+\tau_i-\tau_j-\mathbf{R}_\mathrm{n})\rangle,\end{aligned}$$

$$\mathrm{e}^{-\mathrm{i}\Delta\mathbf{k}\cdot\mathbf{r}'}\approx 1-i\Delta\mathbf{k}\cdot\mathbf{r}'.$$

$$\langle u^{(\mathbf{k})}_{\sigma\mu}|u^{(\mathbf{k}+\Delta\mathbf{k})}_{\sigma\nu}\rangle = \sum_{\mathrm{n}}\sum_{i\alpha,j\beta} c^{(\mathbf{k})*}_{\sigma\mu,i\alpha}c^{(\mathbf{k}+\boldsymbol{\Delta}\mathbf{k})}_{\sigma\nu,j\beta}\mathrm{e}^{\mathrm{i}\mathbf{k}\cdot\mathbf{R}_\mathrm{n}}\mathrm{e}^{-\mathrm{i}\Delta\mathbf{k}\cdot(\tau_i-\mathbf{R}_\mathrm{n})}\times \left\{\langle\phi_{i\alpha}(\mathbf{r}')|\phi_{j\beta}(\mathbf{r}'+\tau_i-\tau_j-\mathbf{R}_\mathrm{n})\rangle - i\Delta\mathbf{k}\cdot\langle\phi_{i\alpha}(\mathbf{r}')|\mathbf{r}'|\phi_{j\beta}(\mathbf{r}'+\tau_i-\tau_j-\mathbf{R}_\mathrm{n})\rangle\right\}$$

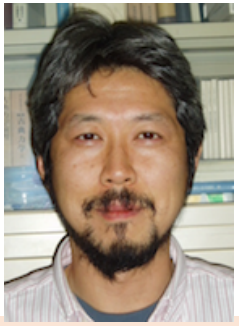

Computing Berry Curvature Chern number and by Fukui-Hatsugai Method

$$\Omega(\mathbf{k}) = (\nabla \times \mathbf{A})_z$$
$$= A_{k_y}(\mathbf{k} + \Delta k_x) - A_{k_y}(\mathbf{k}) - (A_{k_x}(\mathbf{k} + \Delta k_y) - A_{k_x}(\mathbf{k}))$$

$$\mathbf{A}_\mu(\mathbf{k}) = \mathrm{Im} \log U_\mu(\mathbf{k})$$
$$U_\mu(\mathbf{k}) = \langle u(\mathbf{k}) | u(\mathbf{k} + \Delta\mu) \rangle$$

$$U_{ab} = N^{-1} \det \langle u_a | u_b \rangle$$

$$\Omega(\mathbf{k}) = \mathrm{Im} \log U_{12} U_{23} U_{34} U_{41}$$
$$C = \sum_{\mathrm{BZ}} \Omega(\mathbf{k})$$

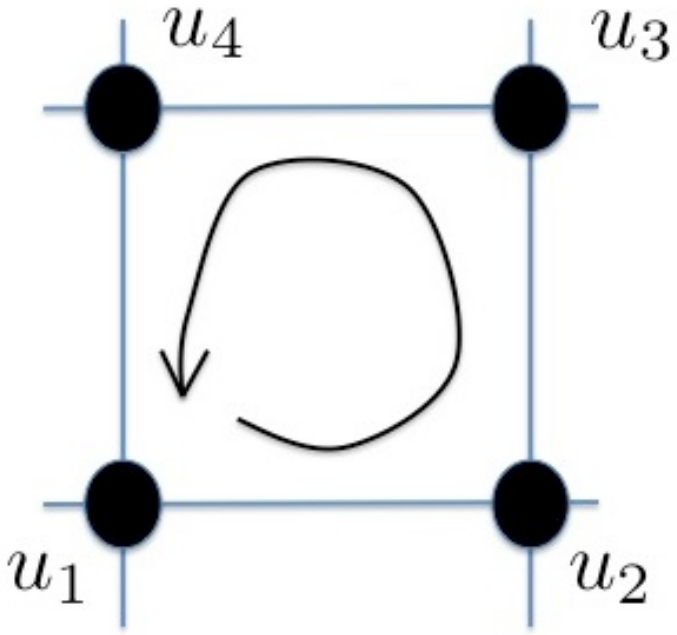

T. Fukui, Y. Hatsugai, and H. Suzuki, J. Phys. Soc. Jpn. **74**, 1674 (2005).

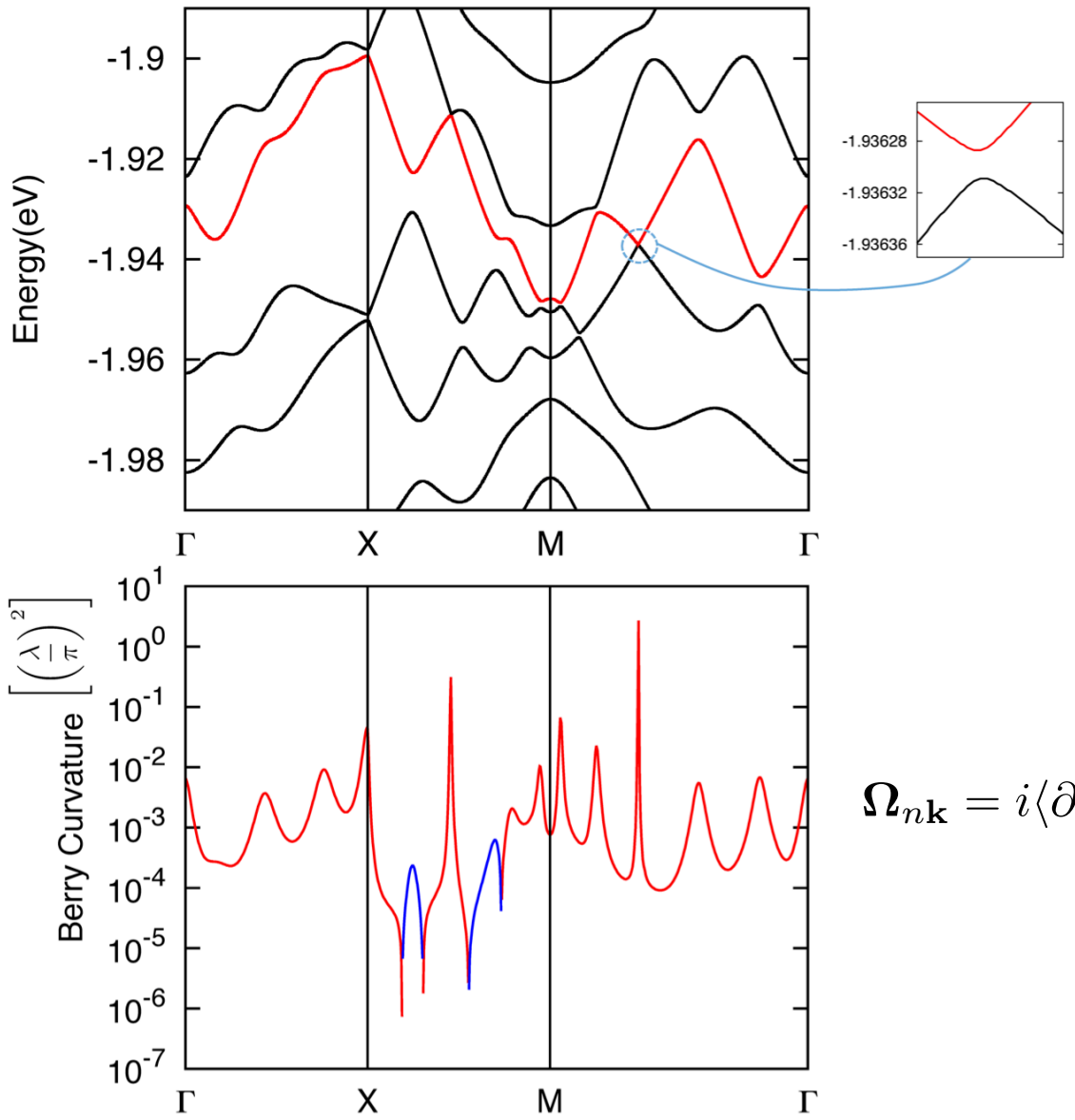

$$\mathbf{\Omega}_{n\mathbf{k}} = i\langle \partial_{\mathbf{k}} u_n | \times | \partial_{\mathbf{k}} u_n \rangle$$

(Top) Band dispersion of central bands and (Bottom) Berry curvature on 21th (from the lowest) band (red line in the top panel) along the path Γ-X-M-Γ. The latter is in logarithmic scale and the red (blue) part indicates its positive (negative) value. The Berry curvature is in unit of $(\lambda/\pi)^2$, where λ is half the value of the lattice constant.

Application

Electric polarization and water dipole moment in ferroelectric ice

Molecular Simulation
Vol. 38, No. 5, April 2012, 369–372

Taylor & Francis
Taylor & Francis Group

First-principles study of spontaneous polarisation and water dipole moment in ferroelectric ice XI

Fumiyuki Ishii[a]*, Kei Terada[b] and Shinichi Miura[a]

[a]*Faculty of Mathematics and Physics, Institute of Science and Engineering, Kanazawa University, Kanazawa 920-1192, Japan;* [b]*Department of Computational Science, Faculty of Science, Kanazawa University, Kanazawa 920-1192, Japan*

(*Received 3 August 2010; final version received 16 October 2010*)

Using density functional calculations, spontaneous polarisation of proton-ordered *ferroelectric* ice XI phase is calculated for the first time. Spontaneous polarisation along the *c*-axis of orthorhombic $Cmc2_1$ structure is calculated to be 21 $\mu C/cm^2$, which corresponds to water dipole moment 3.3 D. We have performed systematic calculation of the water dipole moment in proton-ordered ice without ambiguity.

Keywords: water molecule; ice; density functional theory; electric polarisation; electric dipole moment, electronic structure

Problem: definition of dipole moment in periodic system

- R. Martin (1974)

Knowledge of the charge density in a unitcell is not sufficient to determine the polarization.

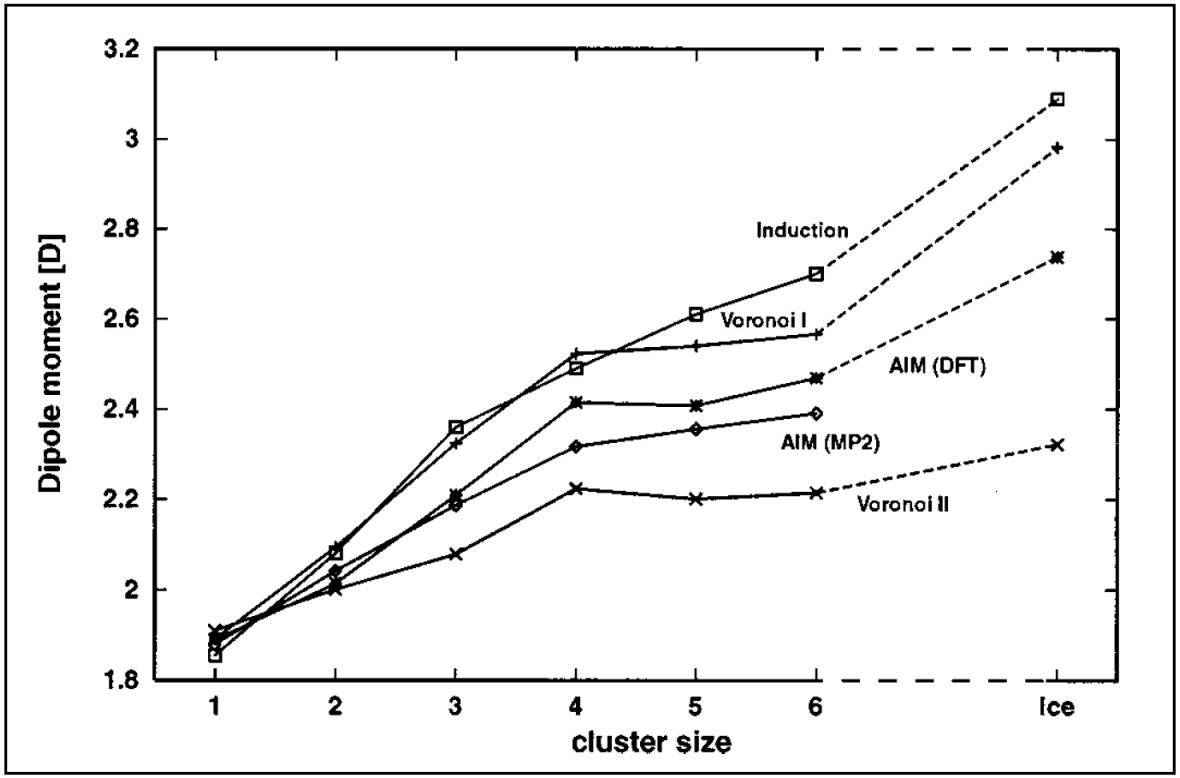

E.R. Batista, S.S. Xantheas, H. Jonsson (J. Chem. Phys. **111**, 6011(1999))

$$\mathbf{P} = \Omega^{-1} \int_{cell} \mathbf{P}(\mathbf{r}) d^3\mathbf{r} \qquad \nabla \cdot \mathbf{P}(\mathbf{r}) = -n(\mathbf{r})$$

$$\mathbf{P} = \Omega^{-1} \int_{cell} \mathbf{r} n(\mathbf{r}) d^3\mathbf{r} + \Omega^{-1} \int_{surface} \mathbf{r}[\mathbf{P}(\mathbf{r}) \cdot d\mathbf{S}]$$

Charge density partition

E.R. Batista, S.S. Xantheas, H. Jonsson
(J. Chem. Phys. **111**, 6011(1999))

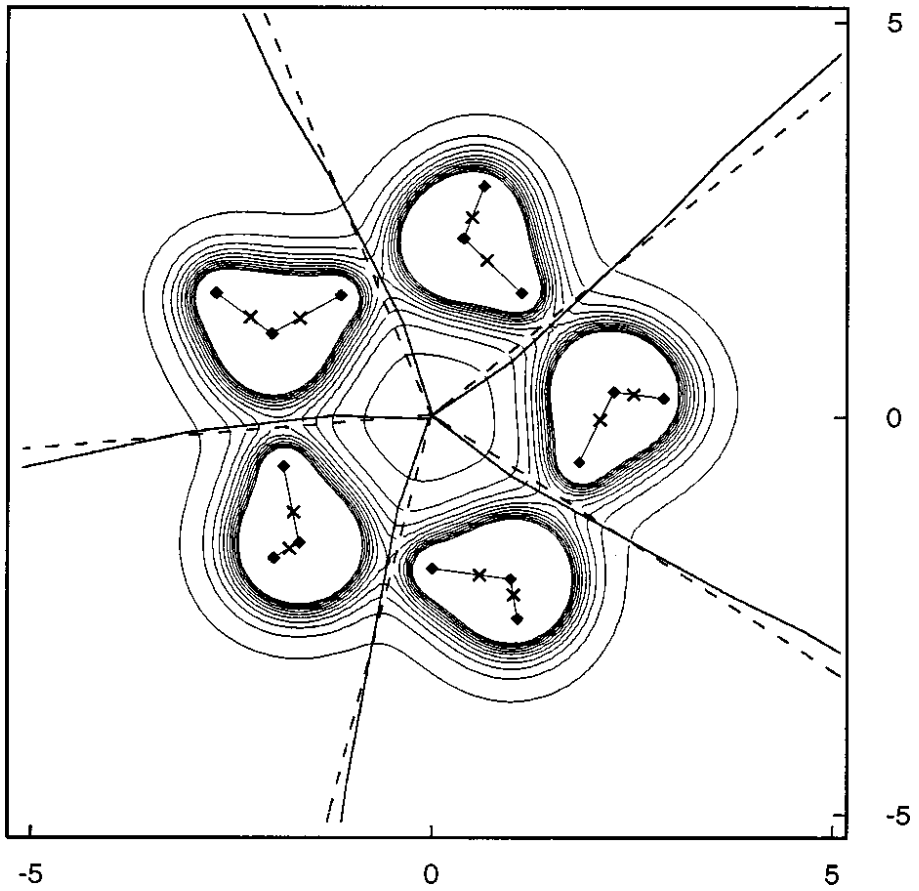

FIG. 1. Contour plot of the charge density of the water pentamer in the plane of the cluster. The figure displays the charge density partitioned according to the Voronoi I (dotted line) and Voronoi II (solid line) schemes (see text). In the Voronoi I scheme, the Voronoi cell is constructed around one center per molecule, placed at the center of nuclear charge. In Voronoi II, the Voronoi cells are around three ''atomic'' centers per molecule: one at the oxygen atom and the other two (shown with crosses) on the O–H bonds, at 40% of the displacement from the oxygen atom to the hydrogen nucleus. Although both surfaces are very similar, the latter passes closer through the minimum of the charge density between the molecules.

F. Ishii, K. Terada, S. Miura, Mol. Siml. **38** 369 (2012).

Charge distribution in ferroelectric ice

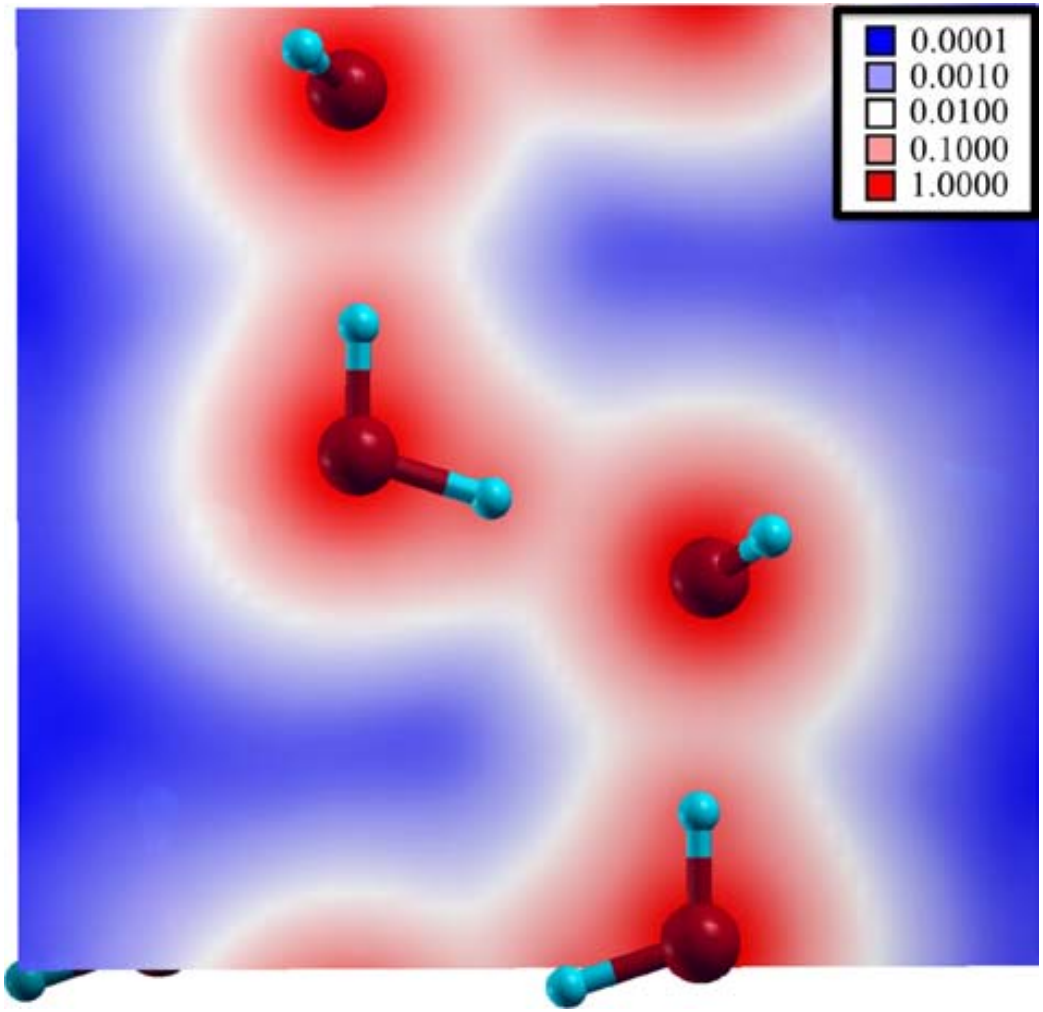

Figure 2. The charge density of ice XI phase viewed from *a*-axis perpendicular to the polarisation direction. Contours are drawn on a logarithmic scale (from 1.0e-4 to 1.0 e/bohr^3).

F. Ishii, K. Terada, S. Miura, Mol. Siml. **38** 369 (2012).

Water dipole moment in hypothetical crystal

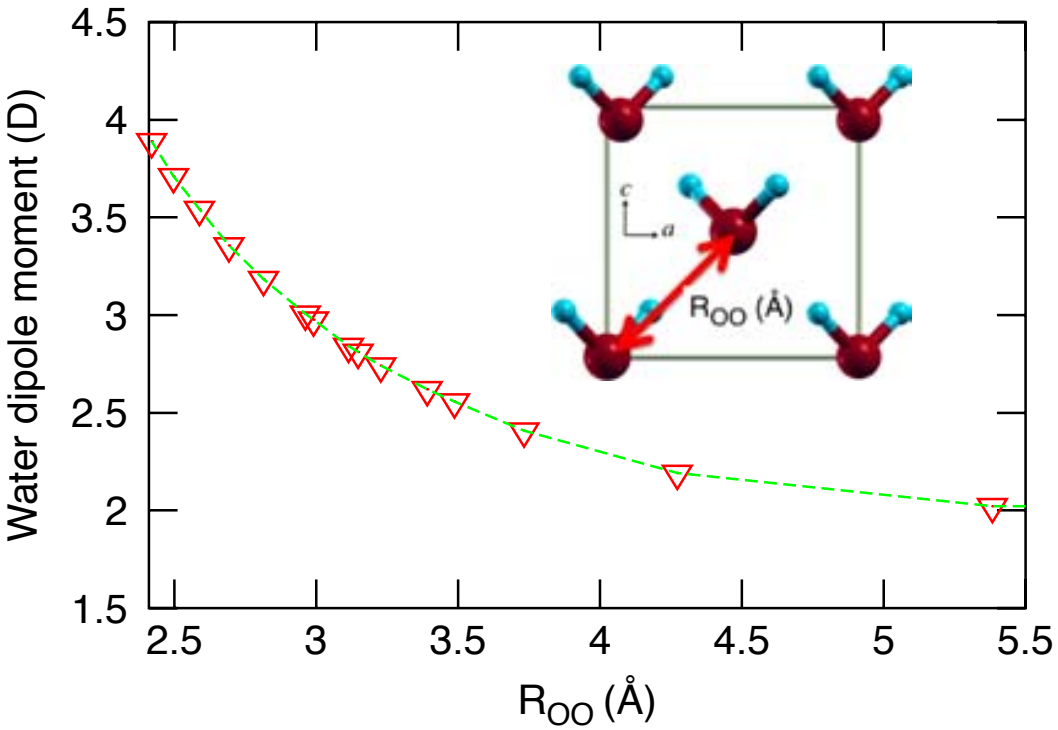

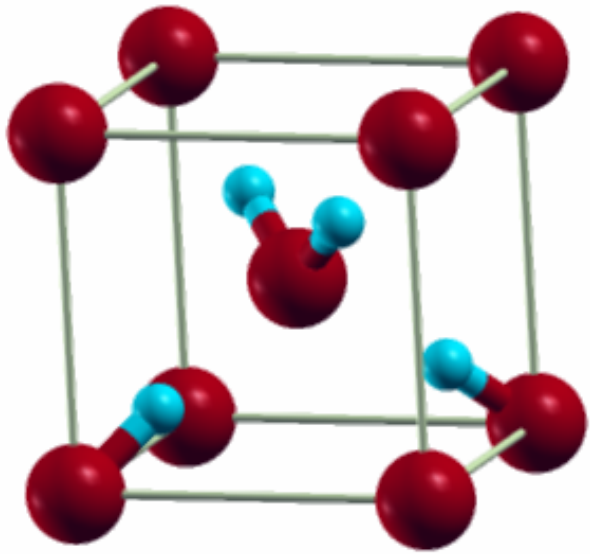

Figure 4. Water dipole moment of model ice with a perspective view of the structure. The triangle indicates water dipole moment versus oxygen–oxygen distance R_{OO}. The lines are a guide to the eye.

Description of Electric polarization in typical ferroelectrics

Hybridization of occupied and unoccupied orbitals under perturbations

Ghosez et al.

Phys. Rev. B 58, 6224(1998)

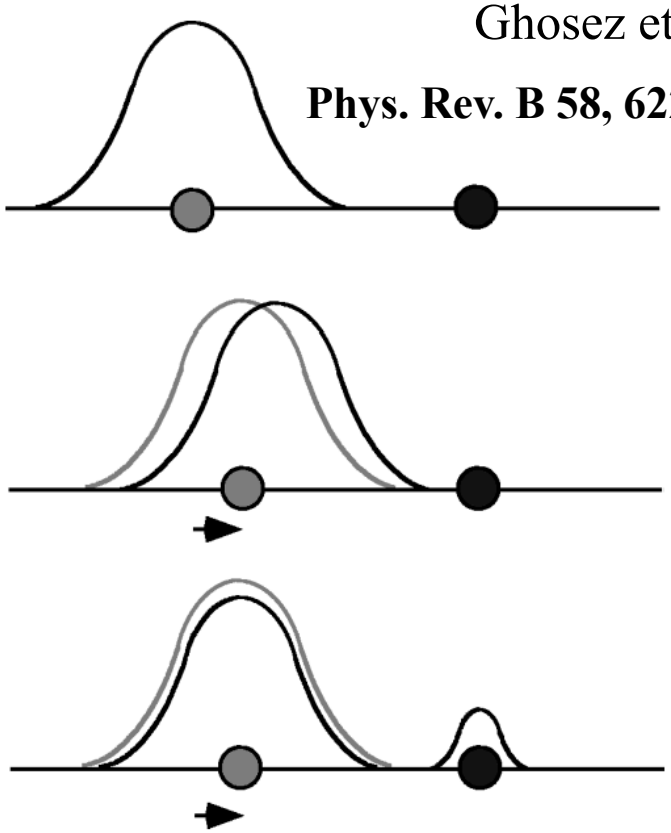

FIG. 2. Schematic representation of the two basic mechanisms that can explain the displacement of the Wannier center of a band under atomic displacement: (middle) local polarizability and (bottom) interatomic transfer of charge.

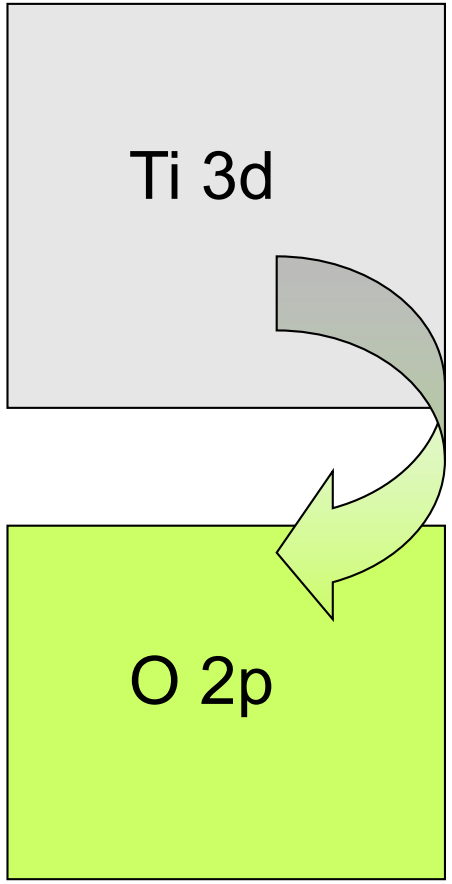

Shift of Wannier function center

nature materials | VOL 4 | FEBRUARY 2005

Ferroelectricity near room temperature in co-crystals of nonpolar organic molecules

SACHIO HORIUCHI[1]*, FUMIYUKI ISHII[2], REIJI KUMAI[1], YOICHI OKIMOTO[1], HIROAKI TACHIBANA[1], NAOTO NAGAOSA[1,3] AND YOSHINORI TOKURA[1,2,3]

[1]Correlated Electron Research Center (CERC), National Institute of Advanced Industrial Science and Technology (AIST), Tsukuba, 305-8562, Japan

[2]Tokura Spin Superstructure Project (SSS), ERATO, JST, c/o AIST, Tsukuba, 305-8562, Japan

[3]Department of Applied Physics, The University of Tokyo, Tokyo 113-8656, Japan

*e-mail: s-horiuchi@aist.go.jp

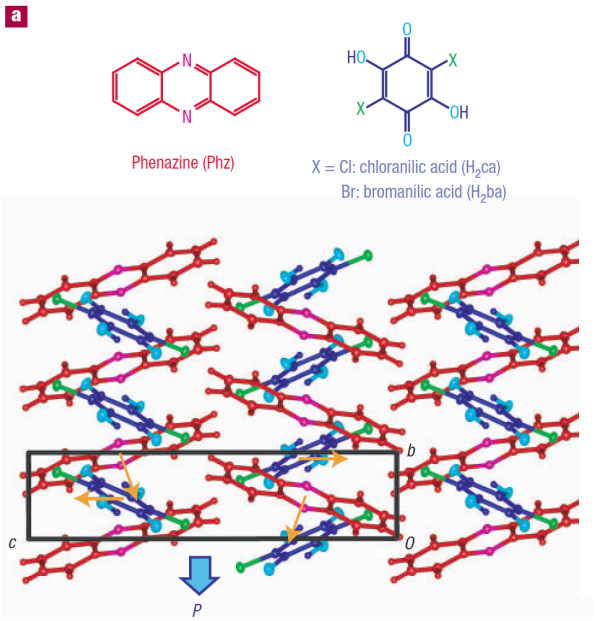

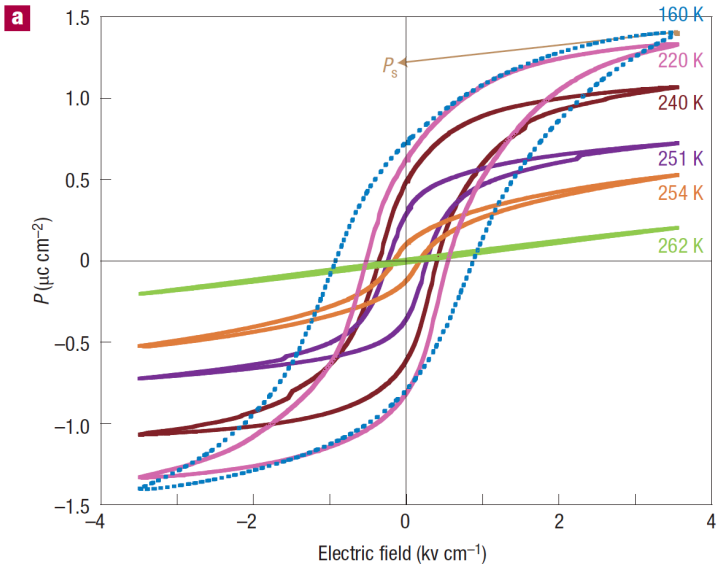

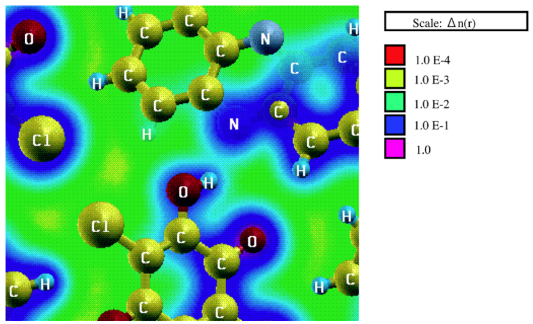

PHYSICAL REVIEW B **73**, 212105 (2006)

Covalent ferroelectricity in hydrogen-bonded organic molecular systems

Fumiyuki Ishii,[1] Naoto Nagaosa,[2,3] Yoshinori Tokura,[1,2,3] and Kiyoyuki Terakura[4]

[1]*Spin SuperStructure Project, ERATO, Japan Science and Technology Corporation, c/o AIST, Tsukuba, 305-8562, Jap*

[2]*Correlated Electron Research Center, AIST, Tsukuba, 305-8562, Japan*

[3]*Department of Applied Physics, University of Tokyo, Tokyo 113-8656, Japan*

[4]*Nanotechnology and Materials Division of Frontier Research, CRIS, Hokkaido University, Sapporo 001-0021, Japa*

(Received 10 November 2005; published 22 June 2006)

We have performed the first-principles calculation on a ferroelectrics phenazine-chloranil acid (Phz-H_2ca), which includes an asymmetric hydrogen bond O-H···N. These hydrogen bonds play the role of building bridges for electronic wave functions between molecules instead of proton tunneling. The charge density in this intermolecular region strongly enhances the electric polarization by the shift of the Wannier function centers, which is described by the Berry phase. It is found that the small molecular distortion enhances the covalency between molecules. This extended nature of electronic wave functions is crucial to the hydrogen-bonded ferroelectrics, which has been ignored in the conventional picture.

$$P_\alpha^{(\lambda)} = (-ief/8\pi^3)\sum_{i=1} \int_{\mathrm{BZ}} d\mathbf{k}\langle u_{i,\mathbf{k}}^{(\lambda)}|\partial/\partial k_\alpha|u_{i,\mathbf{k}}^{(\lambda)}\rangle,$$

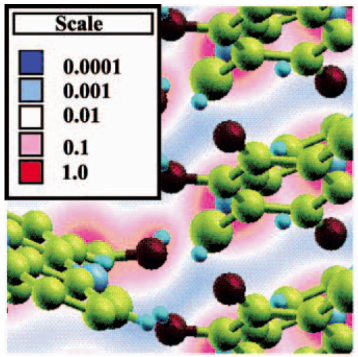

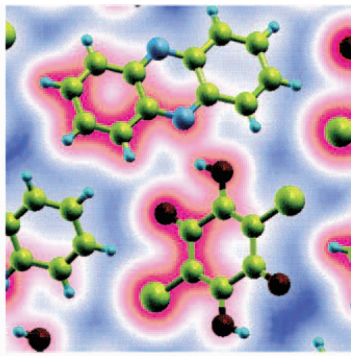

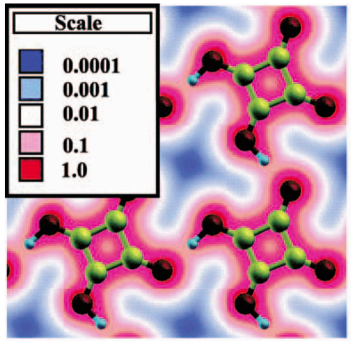

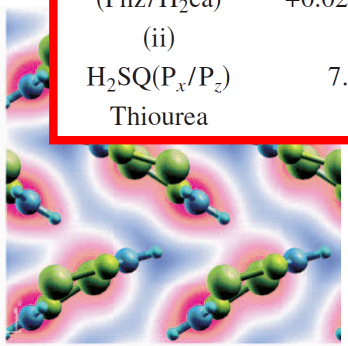

	Molecule	Crystal	Experiment
Phz-H_2ca (i)	0.10	0.32	0.76
(Phz/H_2ca)	+0.029/−0.129		
(ii)		0.55	
H_2SQ(P_x/P_z)	7.5/7.0	17.1/15.8	
Thiourea	2.8	4.9	3.6

Journal of the Physical Society of Japan **83**, 124711 (2014)
http://dx.doi.org/10.7566/JPSJ.83.124711

Magnetism-Driven Electric Polarization of Multiferroic Quasi-One-Dimensional Ca_3CoMnO_6: First-Principles Study Using Density Functional Theory

Miho Nishida[1], Fumiyuki Ishii[2*], and Mineo Saito[2]

[1]*Graduate School of Natural Science and Technology, Kanazawa University, Kanazawa 920-1192, Japan*
[2]*Faculty of Mathematics and Physics, Institute of Science and Engineering, Kanazawa University, Kanazawa 920-1192, Japan*

(Received July 23, 2014; accepted October 14, 2014; published online November 18, 2014)

We have performed first-principles calculations of quasi-one-dimensional Ca_3CoMnO_6 to investigate the origin of the multiferroicity. We revealed the electronic structure and the reversal of the electric-polarization mechanism induced by magnetic structure changes. We found that the electric polarization originates from symmetry breaking due to magnetic ordering in the quasi-one-dimensional Ising spin chains. We further clarified the strong relationship between the magnetic structure and the electric polarization; this is the variation of the magnetic configuration-induced transition mechanism between the ferroelectric state and the ferrielectric states. Our findings are expected to explain the discrepancy between the magnitude of the electric polarization in previous theoretical and experimental studies.

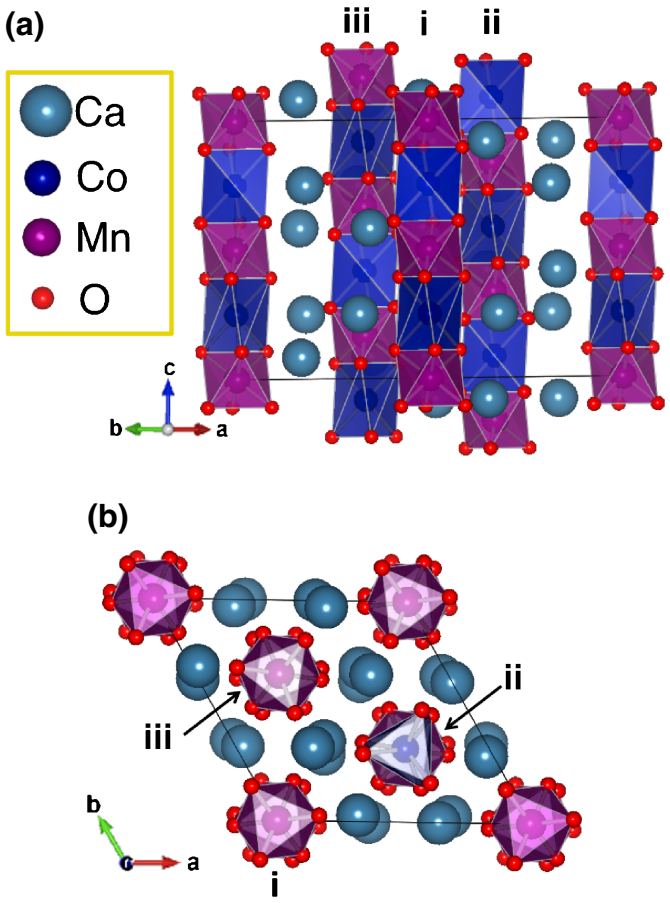

Fig. 1. (Color online) Crystal structure of Ca_3CoMnO_6. The large blue spheres and the small blue spheres represent Ca and Co atoms, respectively. The large magenta spheres and the small red spheres represent Mn and O atoms, respectively. (a) Perspective view from the (110) direction. The blue and magenta shaded areas show the CoO_6 trigonal prism and MnO_6 octahedra, respectively. (i)–(iii) represent the index of the quasi-one-dimensional chains of $(CoMnO_6)_2$. (b) Perspective view from the (001) direction. We see that the quasi-one-dimensional chains are arranged in triangular lattices.

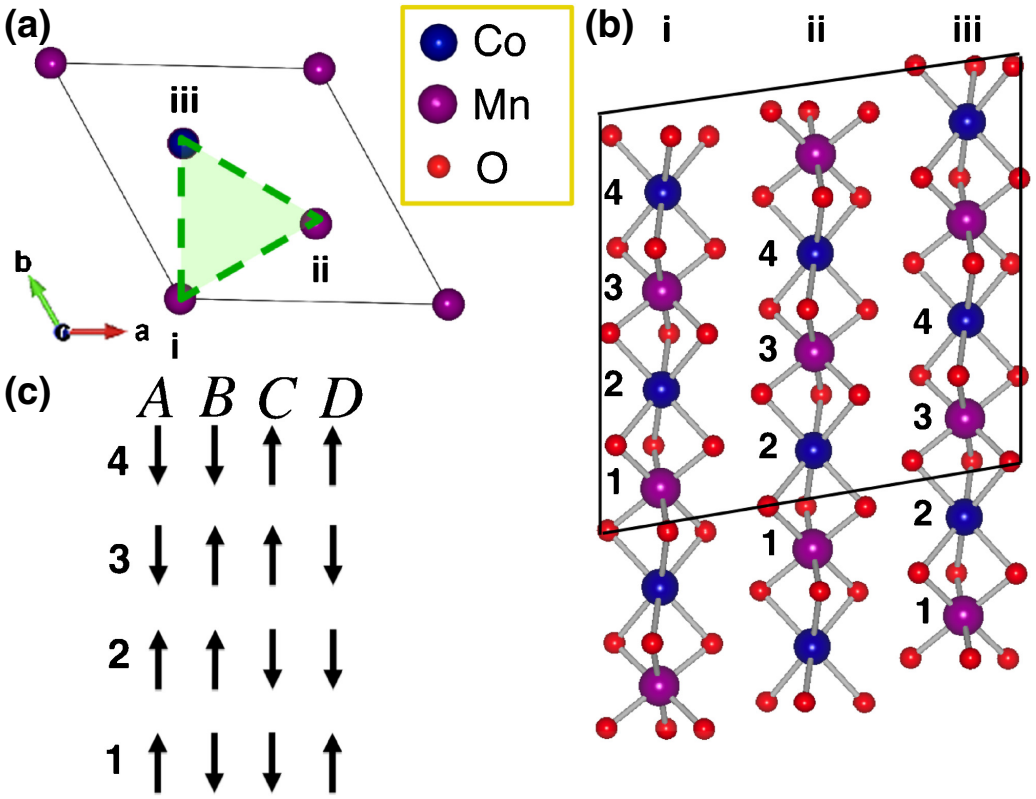

Fig. 2. (Color online) Definition of the spin configurations. (a) Crystal structure viewed from the (001) direction excluding the Ca and O atoms in Fig. 1(b). (b) Three quasi-one-dimensional chains of $(CoMnO_6)_2$. The indices from 1 to 4, at the left side of each chain represent the magnetic atom sites in the intra-chain. The line specifies the atoms in the crystallographic unit cell. The numbers from (i) to (iii) correspond to the lattice sites in (a). (c) The four spin configurations ↑↑↓↓ are indexed from **A** to **D**. The numbers at the left side of the pattern correspond to the numbers in (b).

Table I. Total energy differences ΔE from the most stable magnetic structure. The values in the parentheses denote the total energy difference including SOI. The indices (i, ii, iii) represent the symmetrically equivalent spin configurations of the ↑↑↓↓ magnetic order. The indices from **A** to **D** correspond to the indices in Fig. 2(c). There are 32 possible spin configurations. This list omits spin configurations that invert each spin.

Magnetic structure	(i, ii, iii) Pattern	ΔE (meV/f.u.)
M_0	(A, B, A), (A, C, D), (D, C, A), (B, C, B), (B, D, A), (A, D, B)	0
M_1	(A, C, A), (B, D, B)	+0.10 (0.06)
M_2	(A, A, A), (A, C, C), (C, C, A), (B, B, B), (B, D, D), (D, D, B)	+2.76 (2.71)
M_3	(A, A, B), (B, C, C), (C, D, A), (B, B, C), (C, D, D), (D, A, B)	+2.95 (2.86)
M_4	(A, D, C), (C, C, B), (B, A, A), (B, A, D), (D, D, C), (C, B, B)	+3.43 (3.43)
M_5	(A, D, A), (A, C, B), (B, C, A), (B, A, B), (B, D, C), (C, D, B)	+3.69 (3.61)

Electric polarization

Magnetic Structure	Polarization [μC/m²]
M_5	1227
M_4	1544
M_3	1538
M_2	4316
M_1	3719
M_0	1245

電気分極の値に違い

M_0 and M_1

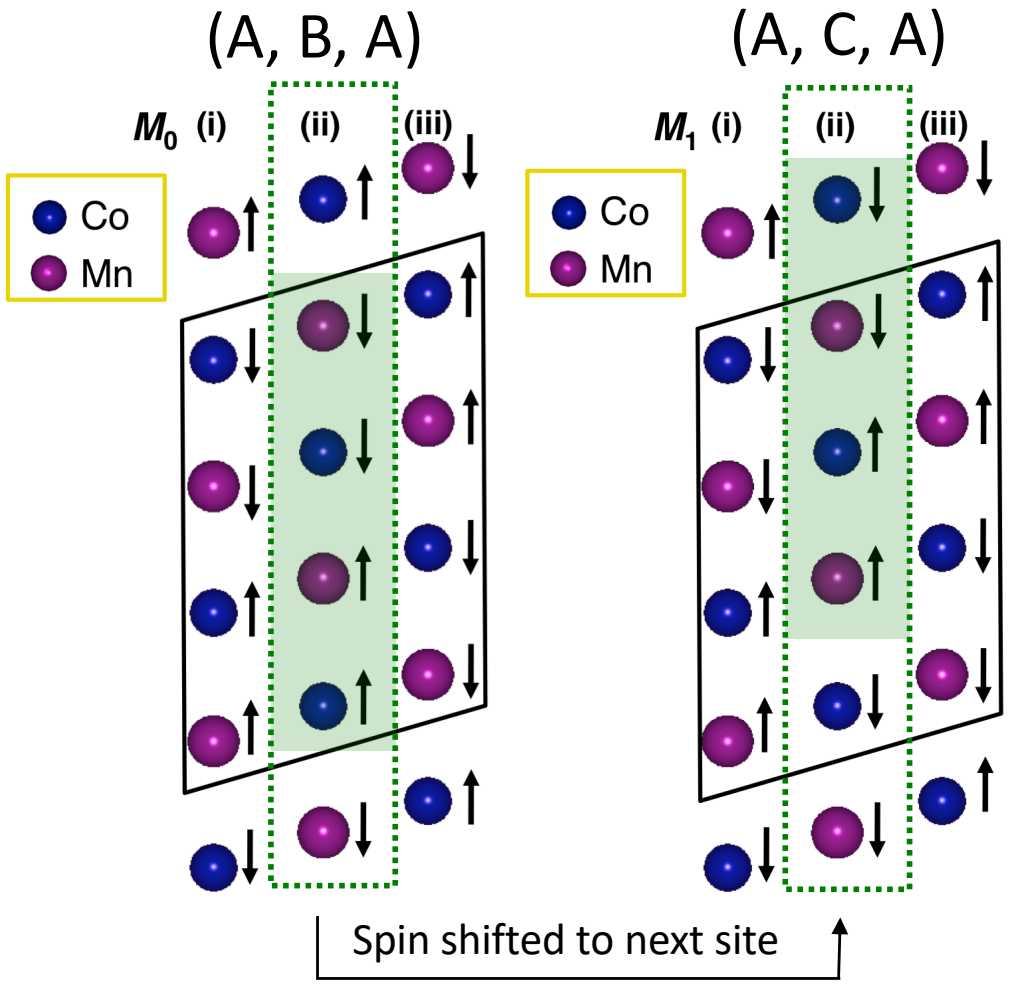

The difference between M_0 and M_1 is magnetic order in (ii) chain.

Electric polarization and Magnetization

Reversal mechanism of ***P***

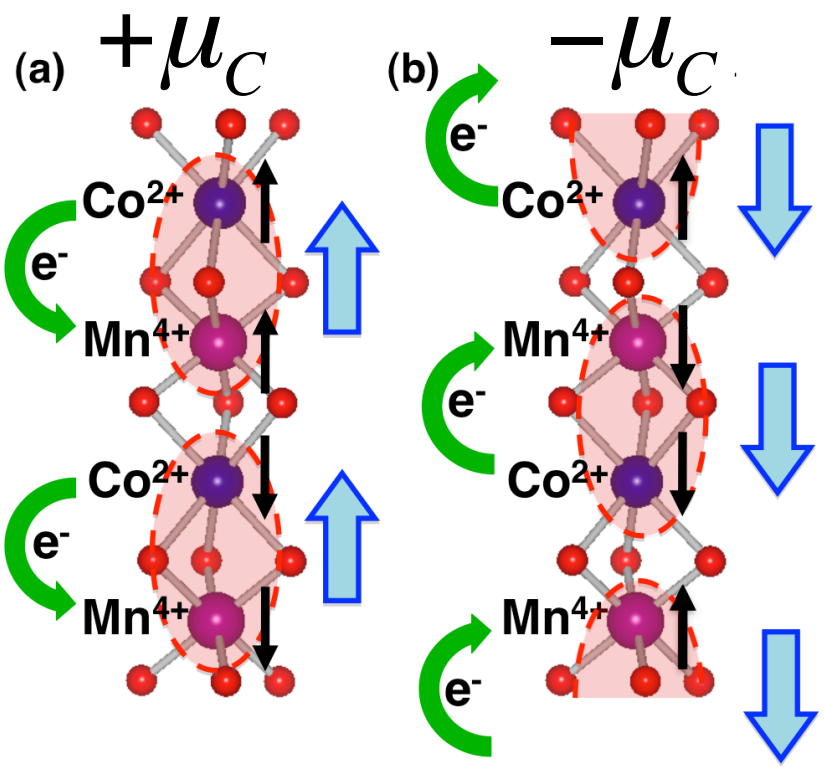

+c direction -c direction

Possible 4 configurations

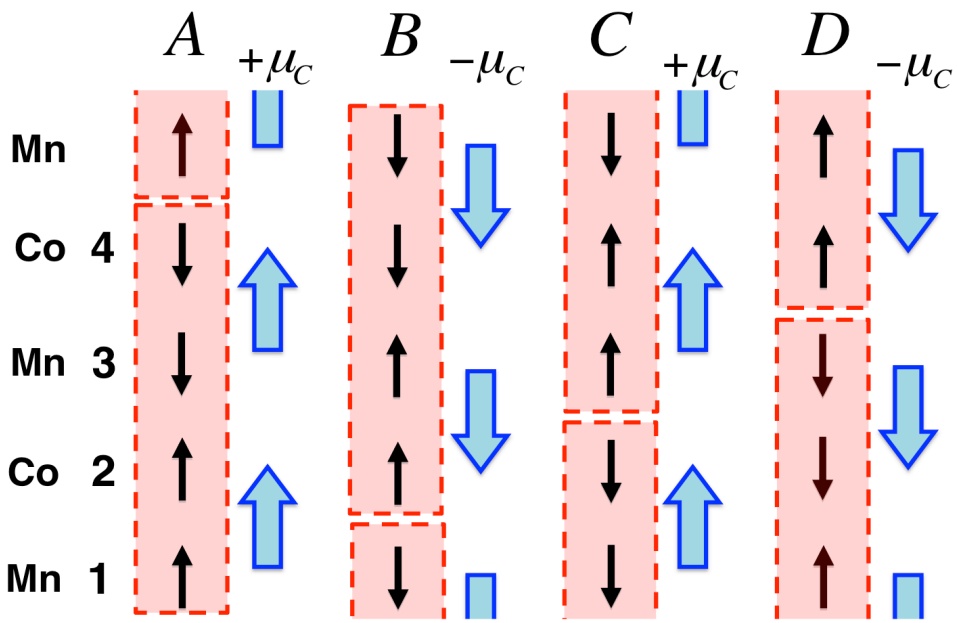

Spin shiftting reverse ***P***

M_0 : (A, B, A) → $1\mu_C/\Omega$ (ferrielectric)

M_1 : (A, C, A) → $3\mu_C/\Omega$ (ferroelectric)

Effective Hamiltonian

Total energy for 4096 spin configuration with symmetry

$$H_{eff} = -\sum_{i<j} J_{ij}\sigma_i\sigma_j$$

Calculating 66 pair of J_{ij}

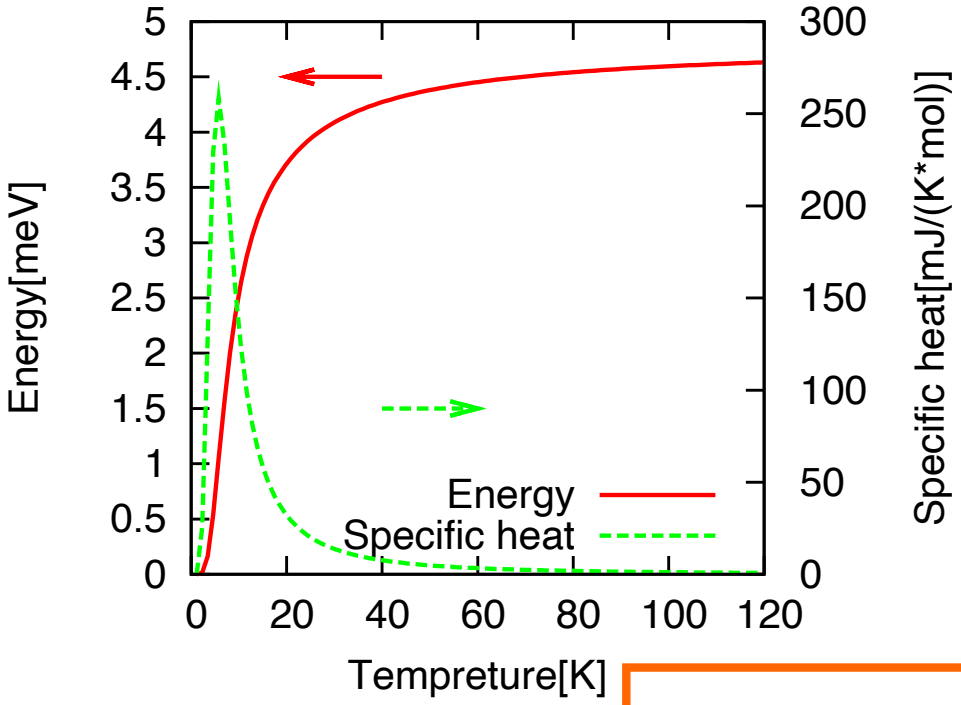

Partition function

$$Z = \sum_{n=1}^{4096} k_n \exp\left(-\frac{E_n}{k_B T}\right)$$

k_n : Degeneracy

E_n : Energy

Expectation value of energy

$$\langle E \rangle = \sum_{n=1}^{4096} k_n E_n \exp\left(-\frac{E_n}{k_B T}\right) / Z$$

Heat capacity

$$\langle C \rangle = \frac{\langle E^2 \rangle - \langle E \rangle^2}{k_B T}$$

Calculated magnetic phase transition at 5.8K.
→Experiment: 16.5K[6]

[6] Y.J. Choi, H.T. Yi, S. Lee et. al., Phys. Rev. Lett., **100**, 047601, (2008).